DMD Fast Forward. Published on July 14, 2011 as DOI: 10.1124/dmd.111.040006
DMD Fast Forward. Published on July 14, 2011 as doi:10.1124/dmd.111.040006
This article has not been copyedited and formatted. The final version may differ from this version.

DMD #40006

Enhancement of oral bioavailability of ginsenoside 20(s)-Rh2 through improved understanding of its absorption and efflux mechanisms

Zhen Yang, Song Gao, Jingrong Wang, Taijun Yin, Yang Teng, Baojian Wu, Ming You, Zhihong Jiang, and Ming Hu

Department of Pharmacological and Pharmaceutical Sciences, College of Pharmacy, University of Houston, 1441 Moursund Street, Houston, TX 77030, USA (ZY,SG,TY,YT,BW,MH)

Medical College of Wisconsin Cancer Center, Medical College of Wisconsin, 8701 West Watertown Plank Road, Milwaukee, WI 53226, USA (MY)

School of Chinese Medicine, Hong Kong Baptist University, 7 Baptist University Road, Kowloon Tong, Hong Kong (JW, ZJ)

Downloaded from dmd.aspetjournals.org at ASPET Journals on April 18, 2024

Copyright 2011 by the American Society for Pharmacology and Experimental Therapeutics.

DMD Fast Forward. Published on July 14, 2011 as DOI: 10.1124/dmd.111.040006
This article has not been copyedited and formatted. The final version may differ from this version.

Running Title: Increase oral bioavailability of Rh2 by inhibition of P-gp

*Address correspondence to:

Ming Hu, Ph.D.

1441 Moursund Street
Department of Pharmacological and Pharmaceutical Sciences
College of Pharmacy, University of Houston
Houston, TX77030
Tel: (713)-795-8320
E-mail: mhu@uh.edu

Number of Text Page:	31
Number of Tables:	2
Number of Figures:	4
Number of References:	35
Number of Words in Abstract:	249
Number of Words in Introduction:	574
Number of Words in Discussion:	1262

Downloaded from dmd.aspetjournals.org at ASPET Journals on April 18, 2024

Abbreviations: Rh2s, ginsenoside 20(s)-Rh2; CsA, cyclosporin A; UPLC, ultra-performance liquid chromatography; P_{a-b}, permeability from apical to basolateral side; P_{b-a}, permeability from basolateral to apical side; P-gp, p-glycoprotein; MDR1, multi-drug resistance gene; MRP2, multidrug resistance associated protein 2; BCRP, breast cancer resistance protein; $AUC_{0-\infty}$, area under the plasma concentration-time curve from time zero to infinity; K_e, constant of elimination rate; $t_{1/2}$, terminal half-life; V_{ss}, apparent volume of distribution at steady state; CL, clearance; F, bioavailability; SIF, simulated intestinal fluid; CYP, cytochrome P450.

DMD Fast Forward. Published on July 14, 2011 as DOI: 10.1124/dmd.111.040006
This article has not been copyedited and formatted. The final version may differ from this version.

Abstract

The development of ginsenoside 20(s)-Rh2 (Rh2s) as a chemoprevention agent is limited by its low oral bioavailability. The goals of this study were to determine the mechanisms responsible for its poor oral absorption and to improve its bioavailability by overcoming the barrier to its absorption. Comprehensive studies were conducted using the following models: 1) monolayers of Caco-2, parental and MDR1 overexpressing MDCKII cells; 2) pharmacokinetics in wild-type (WT) FVB, MDR1a/b knockout (MDR1a/b $^{-/-}$) FVB and A/J mice; and 3) intestinal perfusion in WT, MDR1a/b $^{-/-}$ FVB and A/J mice. Two P-gp inhibitors verapamil and cyclosporin A substantially decreased efflux ratio of Rh2s from 28.5 to 1.0 and 1.2, respectively in Caco-2 cells. The intracellular concentrations of Rh2s were also significantly increased (2.3 and 3.9 fold) in the presence of inhibitors. Similar results were obtained when transcellular transport of Rh2s were determined using MDR1-overexpressing MDCKII cells in the absence or presence of cyclosporin A. Compared to WT mice, the plasma C_{max} and $AUC_{0-\infty}$ of Rh2s were substantially increased by 17 and 23 fold in MDR1a/b $^{-/-}$ FVB mice, respectively. In the A/J mice, the oral bioavailability of Rh2s (0.94% at 5 mg/kg and 0.52% at 20 mg/kg) was substantially increased by P-gp inhibitor to 33.18% and 27.14%, respectively. As expected, deletion or inhibition of P-gp significantly increased absorption and steady-state plasma concentration of Rh2s in a mouse intestinal perfusion model. In conclusion, Rh2s is a good substrate of P-gp and inhibition of P-gp can significantly enhance its oral bioavailability.

Downloaded from dmd.aspetjournals.org at ASPET Journals on April 18, 2024

DMD Fast Forward. Published on July 14, 2011 as DOI: 10.1124/dmd.111.040006
This article has not been copyedited and formatted. The final version may differ from this version.

Introduction

Ginseng is a promising candidate for cancer chemoprevention based on preclinical and epidemiological studies (Yun, 1996; Helms, 2004; Varjas et al., 2009). In a case-controlled study including 1987 pairs of Korean subjects, the long-term consumption of ginseng was shown to be associated with a significant reduction in many different types of malignancies including lung cancer (Yun, 2003). Ginsenosides are the main active components of ginseng and there are more than 100 ginsenosides identified so far (Christensen, 2009). The chemoprevention and anticancer mechanism of ginsenosides include mitigation of DNA damage, induction of apoptosis, and inhibition of proliferation as well as positive immunomodulation (Helms, 2004).

However, extensive pharmacokinetic studies indicated that many active ginsenosides have very poor oral bioavailability (much less than 5%), which had been attributed to poor oral absorption (Gu et al., 2009; Liu et al., 2009). Poor bioavailability of ginsenosides greatly impedes our ability to demonstrate the potency of ginsenosides in vivo, and our ability to overcome this impediment perhaps holds the key to advance these agents into clinical trials that will unequivocally demonstrate their clinical effectiveness (Coleman et al., 2003; Buettner et al., 2006; Jia et al., 2009).

In this study, ginsenoside 20(s)-Rh2 (Rh2s) was selected as a lead compound to demonstrate the absorption mechanisms of ginsenosides. Ginsenoside Rh2s is one of the most studied ginsenosides since it displayed potent anticancer activity, especially in lung cancer cell lines (Cheng et al., 2005; Wang et al., 2006). A 9-week animal study also showed Rh2s had a tendency to decrease lung tumor incidence in mice after its oral consumption (Yun, 2003). Like many other ginsenosides, Rh2s was reported as having low oral absorption/bioavailability (Qian et al., 2005; Gu et al., 2009). However, current understanding of Rh2s absorption mechanism is

Downloaded from dmd.aspetjournals.org at ASPET Journals on April 18, 2024

DMD Fast Forward. Published on July 14, 2011 as DOI: 10.1124/dmd.111.040006
This article has not been copyedited and formatted. The final version may differ from this version.

ambiguous. Gu et al. reported that ABC efflux transporters may be involved in Rh2s absorption, but no actual transporter was identified (Gu et al., 2010). The latest publication from the same group found that Rh2s was a non-competitive inhibitor but not a substrate of P-gp (Zhang et al., 2010). Therefore, identification of the predominant transporter for Rh2s and demonstration that the inhibition of relevant efflux transporters would increase oral bioavailability of Rh2s (and maybe other ginsenosides) would help us to further understand and delineate this class of compounds' pharmacological characteristics.

P-glycoprotein (P-gp), a member of the adenosine triphosphate (ATP)-binding cassette (ABC) superfamily, is one of the most prevalent efflux transporters expressed in multidrug resistance cancer cells and in several organs such as intestine, liver, kidney and the blood-brain barrier (Sharom, 2008). P-gp plays an important role in limiting the intestinal absorption of its substrates in vivo (Kusuhara and Sugiyama, 2002) and inhibition of P-gp leads to the improvement of bioavailability of several orally administrated anticancer drugs (Meerum Terwogt et al., 1998; Kemper et al., 2004; van Waterschoot et al., 2009). Most P-gp substrates are hydrophobic, and a recently published mouse P-gp crystal structure revealed that P-gp has distinct drug-binding sites (in the large internal activity cavity) favoring hydrophobic and aromatic interactions (Aller et al., 2009).

Therefore, the aims of this study were 1) to systemically investigate mechanisms responsible for poor absorption of Rh2s by elucidate which efflux transporter was mainly involved in the transport of Rh2s using a complementary set of *in vitro*, *in situ* and *in vivo* models; 2) to demonstrate that it is possible to increase oral bioavailability of Rh2s via a mechanism-based approach (i.e., focus on inhibiting the elucidated efflux transporter derived from aim 1).

Downloaded from dmd.aspetjournals.org at ASPET Journals on April 18, 2024

DMD Fast Forward. Published on July 14, 2011 as DOI: 10.1124/dmd.111.040006
This article has not been copyedited and formatted. The final version may differ from this version.

Materials and Methods

Chemicals and reagents

Purified Rh2s (HPLC purity>95%, Fig. 1) were prepared by Dr. Zhi-Hong Jiang's laboratories at Hong Kong Baptist University. Cloned Caco-2 cells (TC7) cells were a kind gift from Dr. Monique Rousset of INSERM U178 (Villejuit, France). Parental MDCKII and MDR1-MDCKII cells were provided by the Netherland Cancer Institute (Amsterdam, Netherland). Digoxin, cyclosporin A, verapamil and Hanks' balanced salt solution (powder form) were purchased from Sigma-Aldrich (St. Louis, MO). MK571 and Ko143 were purchased from Tocris Bioscience (Ellisville, MO). Oral suspension vehicle was obtained from Professional Compounding Centers of America (Houston, TX). Simulated intestinal fluid was purchased from VWR (Houston, TX). BCA protein assay kit was purchased from Thermo Scientific (Rockford, IL). All other materials (typically analytical grade or better) were used as received.

Animals

Male A/J and FVB mice (6-10 weeks) were purchased from Harlan Laboratory (Indianapolis, IN). Male MDR1a/b knockout mice (6-10 weeks) were purchased from Taconic Farms (Germantown, NY). They were acclimated in an environmentally controlled room (temperature: 25 ± 2°C, humidity: 50 ± 5%, 12 h dark-light cycle) for at least 1 week prior to experiments. The mice were fed with rodent diet (Labdiet® 5001), and fasted overnight before pharmacokinetic studies.

Cell culture

The Caco-2 cell culture is routinely maintained in this laboratory for the last 2 decades. The culture conditions for growing Caco-2 cells were the same as those described previously (Yang et al., 2010a). Porous polycarbonate cell culture inserts (3 µm) from Corning (Catalog No: 3414)

Downloaded from dmd.aspetjournals.org at ASPET Journals on April 18, 2024

DMD Fast Forward. Published on July 14, 2011 as DOI: 10.1124/dmd.111.040006
This article has not been copyedited and formatted. The final version may differ from this version.

were used to seed the cells at a seeding density of 100,000 cells/cm^2. Other conditions such as growth media (Dulbecco's modified Eagle's medium supplemented with 10% fetal bovine serum), and quality control criteria were all implemented according to a previous published report (Yang et al., 2010a) . Caco-2 TC7 cells were fed every other day, and cell monolayers were ready for experiments from 19 to 22 days post-seeding.

Parental MDCKII and MDR1-MDCKII cells were cultured in Dulbecco's modified Eagle's medium supplemented with 10% fetal bovine serum, 1% nonessential amino acids, 100U/ml penicillin and gentamicin. Cell culture was maintained at 5% CO_2 and 90% relative humidity at 37°C. They were seeded at 2.0×10^6 cells/well into the same cell culture inserts as those used for Caco-2 cells, and fed every day. The MDCKII or MDR1-MDCKII cell monolayers were ready for experiments from 4-5 days post-seeding. The expression levels of MDR1 in MDR1-MDCKII were monitored by western blotting analysis.

Saturated aqueous solubility measurement

Ginsenoside Rh2s is a strong lipophilic (log P=4.0, predicted by Molecular Operating Environment and Discovery Studios) compound and its solubilities in various media had not been reported. HBSS buffer was commonly used in absorption models including the Caco-2 cells and in situ rodent intestinal perfusion study (Yang et al., 2010b). The saturated aqueous solubility was measured in HBSS using pH values ranging from pH 5.5 to pH 8.0. The solubility of Rh2s was also determined in pure water at pH 7.4 and in simulated intestinal fluid (SIF) at pH 6.8 to mimic the in vivo environment. Stock solution of ginsenoside Rh2s was prepared in alcohol at 10 mM. 10 µl of Rh2s was spiked into glass vials in triplicate and dried under air. A volume of 1 ml HBSS/water/SIF at appropriate pH values was then added into a glass vial and the mixture was shaken overnight at 37°C. After the mixture was centrifuged at 15,000 rpm for 20 minutes, 400 µl of supernatant was then carefully transferred into a new vial. The vial was

Downloaded from dmd.aspetjournals.org at ASPET Journals on April 18, 2024

DMD Fast Forward. Published on July 14, 2011 as DOI: 10.1124/dmd.111.040006
This article has not been copyedited and formatted. The final version may differ from this version.

then added with 100 µl formononetin (10 µM) as the internal standard (I.S.) and dried under air. The residue was reconstituted with 200 µl methanol and centrifuged at 15,000 rpm for 10 minutes. A volume of 10 µl supernatant was injected to UPLC-MS/MS for analysis.

Transcellular transport study

The transcellular transport study was performed as described previously (Yang et al., 2010a). Briefly, 2.5 ml of Rh2s solution was loaded onto one side of the cell monolayer, and 2.5 ml of blank HBSS onto the other side. Five sequential samples (0.5 ml) were taken at different times (0, 1, 2, 3 and 4 hrs) from both sides of the cell monolayer. The same volume of Rh2s solution and receiver medium (fresh HBSS) was added immediately to replace the volume lost because of sampling. The pH values of HBSS in both apical and basolateral side were 7.4. The apparent unidirectional permeability was obtained according to the following equation (Eq.1):

$$\mathrm{P_{app}} = \frac{dC}{dt} \times \frac{V}{\mathrm{SC_0}} \qquad (1)$$

where $\frac{dC}{dt}$ is the rate of concentration change in the receiver chamber (equals to the slope of the regression line derived for the amount transported vs. time profile), V is the chamber volume (2.5 ml), S is the surface area of the monolayer (4.65 cm^2), and C_0 is the starting concentration in the donor side.

Both permeability from apical to basolateral side ($P_{a\text{-}b}$) and basolateral to apical side ($P_{b\text{-}a}$) were calculated according to the above equation. Digoxin, a substrate of P-gp, was used as the positive control for the transport study in Caco-2 and MDR1-MDCKII cell monolayers. The efflux ratio was calculated as $P_{b\text{-}a}/P_{a\text{-}b}$, which represented the degrees of efflux transporter involvement. In the present study, inhibitors of efflux transporters were only added to the apical side of cell monolayers, regardless of where Rh2s was loaded.

Downloaded from dmd.aspetjournals.org at ASPET Journals on April 18, 2024

DMD Fast Forward. Published on July 14, 2011 as DOI: 10.1124/dmd.111.040006
This article has not been copyedited and formatted. The final version may differ from this version.

Intracellular concentrations of Rh2s were determined at the end of a transport study. The protocol for determining Rh2s intracellular amounts in cells was the same as those described previously (Jeong et al., 2005). Briefly, after 4 hours of a transcellular transport study, the cell membranes were rinsed three times with ice-cold HBSS buffer, and cells attached to the polycarbonate membranes were cut off from the inserts with a sharp blade. The latter was immersed into 1 ml HBSS, and sonicated for half an hour at 4°C to break up the cells. The mixture was centrifuged at 15,000 rpm for 15 minutes and 500 µl of the supernatant were recovered and air-dried. The residue were reconstituted with 200 µl methanol and analyzed by UPLC-MS/MS. The protein concentration of cell lysate was measured to normalize the accumulation of Rh2s inside the cells using the BCA protein assay kit.

In situ two-site mouse intestinal perfusion study

The animal protocols used in this study were approved by the University of Houston's Institutional Animal Care and Uses Committee. The intestinal surgical procedures were described in our previous publications (Jeong et al., 2005). Two segments of intestine, upper small intestine and colon (8-12cm each) were simultaneously cannulated. The perfusion studies were performed at a flow rate of 0.191 ml/min with 2 µM Rh2s in HBSS iso-osmotic solution (pH 7.4) using A/J, WT and MDR1a/b $^{-/-}$ FVB mice. Cyclosporin A solution (10 µM) was mixed with 2 µM Rh2s in A/J mice to test the effects of P-gp inhibitors on Rh2s transport. To keep the temperature of the perfusate constant, the inlet cannulate was insulated and kept warm by a 37°C circulating water bath.

After a 30 min washout period with perfusate, perfusate samples were collected every 30 min (60, 90, 120, 150 min). At the end of the perfusion experiment, the length of the each segment of intestine was measured and each tube containing sample was weighted after perfusion. 50 µl of blood was collected from tail vein at the end of perfusion experiment (2.5 hr

Downloaded from dmd.aspetjournals.org at ASPET Journals on April 18, 2024

DMD Fast Forward. Published on July 14, 2011 as DOI: 10.1124/dmd.111.040006
This article has not been copyedited and formatted. The final version may differ from this version.

after the start). Loss of water during perfusion was monitored by measuring the net weight of perfusate sample and the absorption data was discarded if the water flux is more than 5% per 10 cm for the small intestine and 10% per 10 cm for the colon. The perfusate samples were immediately processed the same way as the cellular transport samples, and analyzed by UPLC-MS/MS. The plasma concentrations of Rh2s were measured following the same protocol in pharmacokinetic study. The percentages of absorption were calculated using the equation (2):

$$\text{Absorption } \% = \left(1 - \frac{C_{out}}{C_{in}}\right) \times 100\% \qquad (2)$$

In equation (2), C_{out} and C_{in} are outlet and inlet perfusion concentrations of Rh2s after correcting for water fluxes, respectively.

Stability of Rh2s in blank perfusate was measured to ensure that the concentration disappeared from the intestinal perfusate was due to absorption. Rh2s was spiked into fresh blank perfusate (final concentration =2 μM) collected from upper small intestine and colon of A/J mice and immediately put into a rotating water bath (40 rpm) at 37°C to mimic in vivo conditions. After 0, 1, 2, 4 and 8 h, 0.5 ml of the incubated fluids were collected and their concentrations were determined as described above.

Pharmacokinetic studies of Rh2s in wild-type and MDR1a/b $^{-/-}$ FVB Mice

Pharmacokinetic studies of Rh2s were performed in wild-type and MDR1a/b $^{-/-}$ FVB mice to confirm the role of MDR1/P-gp in determining Rh2s bioavailability in vivo. Rh2s dispersed in the oral suspending vehicle (Supplemental Table 1) was given by gavage to each group at 20 mg/kg. Each pharmacokinetic study was performed on five mice and 10 timed blood samples (20-25 μl) were taken by snipping its tail, after mice were anesthetized with isoflurane gas. The blood samples were collected in heparin treated tubes and stored at -20°C until analysis.

Downloaded from dmd.aspetjournals.org at ASPET Journals on April 18, 2024

DMD Fast Forward. Published on July 14, 2011 as DOI: 10.1124/dmd.111.040006
This article has not been copyedited and formatted. The final version may differ from this version.

Pharmacokinetic studies of Rh2s alone or with cyclosporin A in A/J mice

Pharmacokinetic studies of Rh2s were performed in A/J mice for both i.v. and oral administrations. Rh2s (1 mg/ml) was prepared in 20% alcohol and 20% propylene alcohol in normal saline and was intravenously injected through lateral tail vein at the dose of 5 mg/kg. In oral dosing groups without cyclosporin A (control group), 4 mg/ml Rh2s was dispersed in oral suspending vehicle and the content of Rh2s in oral suspending vehicle was measured before administration to make sure it was evenly suspended. The ingredients of oral suspending vehicle are shown in Table S1. In the group with co-administration of P-gp inhibitors, 50 mg/kg solid cyclosporin A dispersed in the same oral suspending vehicle was orally administrated to A/J mice 30 minutes before Rh2s administration while the same volume of blank vehicle was given to the control group. The blood sample collection and processing procedures used for A/J mouse samples were the same as those described for the FVB mouse pharmacokinetic study.

Sample Processing and Quantitative Determination of Rh2s

An API 3200 Qtrap® triple quadrupole mass spectrometer (Applied Biosystems/MDS SCIEX, Foster City, CA, USA) equipped with a TurboIonspray™ source, operated in a negative ion mode, was used to perform the analysis of the eluent from the UPLC.

The flow dependent parameters for introduction of the samples to the mass spectrometers ionization source were set as follows: ion spray voltage, -4.5 kV; ion source temperature, 650°C; the nebulizer gas (gas1), nitrogen, 50 psi; turbo gas (gas2), nitrogen, 50 psi; curtain gas, nitrogen, 10 psi.

The quantification was performed using multiple reactions monitoring mode (MRM) with ion pair transitions to monitor Rh2s and formononetin (Internal standard). The fragments for each compound detected were 621.4/160.9 (m/z) for Rh2s and 267.1/252.1 (m/z) for formononetin.

Downloaded from dmd.aspetjournals.org at ASPET Journals on April 18, 2024

DMD Fast Forward. Published on July 14, 2011 as DOI: 10.1124/dmd.111.040006
This article has not been copyedited and formatted. The final version may differ from this version.

UPLC conditions for Rh2s analysis were: system, Waters Acquity™ (Milford, MA, USA) with DAD detector; column, Acquity UPLC BEH C18 column (50×2.1mm I.D., 1.7μm, Waters); mobile phase A, double distilled water; mobile phase B, 100%, methanol; gradient, 0-0.5 min, 0% B, 0.5-1 min, 0-80% B, 1-2.3 min, 80-95% B, 2.3-2.9 min, 95% B, 2.9-3.2 min, 95-0% B, 3.2-3.7 min, 0% B. Flow rate, 0.45 ml/min, column temperature, 60 degree; injection volume, 10 μl. The chromatograph of Rh2s and I.S. is shown in Supplemental Figure 1.

The standard curves of Rh2s were linear in the concentration range of 0.0195-10 μM and the LLOQ was 0.00975 μM in blood. The intra-day and inter-day precision were within 15% for all QC samples at three concentration levels (2.5, 0.3125 and 0.039 μM). The mean extraction recoveries determined using three replicates of QC samples at three concentrations in mouse blood were from 55.8 to 67.0%. The stability of Rh2s in mouse blood were evaluated by analyzing three replicates of quality control samples after short-term (25°C, 4h), post processing (20°C, 8h), long-term cold storage (-20°C, 7days) and within three freeze-thaw cycles (-20 to 25°C). All the samples displayed 85-115% recoveries after various stability tests.

Quantification of digoxin (positive control in Rh2s transport studies) was performed in UPLC-MS/MS with the same instrumental conditions used for analysis of Rh2s. The detailed compound-dependent mass spectrometer parameters were shown in Supplemental Table 2.

Before samples could be introduced into the UPLC, they were processed to remove proteins and other related substances. A volume of 200 μl methanol (containing 1 μM formononetin) was added into 20 μl aliquot of mouse blood sample. The sample mixtures were vortexed for about 30 seconds and precipitates were removed by centrifugation at 15,000 rpm for 15 min. The supernatant was transferred into a clean glass vial and evaporated to dryness at 40°C under air. The dry residue was reconstituted in 100 μl of 100% methanol (v/v), and a 10 μl aliquot of the resulting solution was injected into the UPLC-MS/MS system for analysis.

Downloaded from dmd.aspetjournals.org at ASPET Journals on April 18, 2024

DMD Fast Forward. Published on July 14, 2011 as DOI: 10.1124/dmd.111.040006
This article has not been copyedited and formatted. The final version may differ from this version.

Pharmacokinetic analysis

WinNonlin 3.3 (Pharsight Corporation, Mountain View, California) was used for Rh2s pharmacokinetic analysis. The non-compartmental model was applied for pharmacokinetic analysis of Rh2s profiles. Pharmacokinetic parameters, including C_{max}, T_{max}, k_e, half-life and AUC were directly derived from WinNonlin. The absolute oral bioavailability (F) was calculated by the following equation (3):

$$F\% = \frac{Dose_{i.v.}AUC_{p.o.}}{Dose_{p.o.}AUC_{i.v.}} \times 100\% \quad (3)$$

The clearance and apparent volume of distribution at steady state after oral administration were corrected from the original CL (CL_o) and V_{ss} (V_{sso}) obtained from WinNonlin using the F values, as shown in equations (4 & 5).

$$\mathrm{CL} = F \times \mathrm{CL_o}/100 \quad (4)$$

$$V_{ss} = F \times \mathrm{V_{ss_o}}/100 \quad (5)$$

Statistical analysis

The data in this paper were presented as means ± S.D., if not specified otherwise. Significance differences were assessed by using Student's t-test or one-way ANOVA. A p value of less than 0.05 or $p<0.05$ was considered as statistically significant.

Downloaded from dmd.aspetjournals.org at ASPET Journals on April 18, 2024

DMD Fast Forward. Published on July 14, 2011 as DOI: 10.1124/dmd.111.040006
This article has not been copyedited and formatted. The final version may differ from this version.

Results

Saturated aqueous solubility

We measured the saturated aqueous solubility of Rh2s in HBSS at different pHs. The results showed that Rh2s had low aqueous solubilities in HBSS buffer (1.9 ± 0.2, 2.0 ± 0.2, 2.9 ± 0.2, 2.4 ± 0.4 μg/ml) at four tested pH values (5.5, 6.5, 7.4 and 8.0), respectively. There was no significant difference in solubility at different pH values according to a one-way ANOVA analysis. The concentrations of Rh2s in saturated solutions were 5.4 ± 0.4 μg/ml in pure water (pH 7.4), and 7.2 ± 2.5 μg/ml in simulated intestinal fluid (pH 6.8), respectively. Consistent with the solubility results, we found visible precipitates in the HBSS samples when trying to reach concentrations above 10 μM (6.22 μg/ml) after centrifugation. In contrast, the solutions were clear in the blank HBSS buffer or in samples with lower concentrations of Rh2s. The measured solubility of Rh2s in those three matrixes indicated that Rh2s has a limited aqueous solubility, which also limits the maximal concentration that could be used for in vitro transcellular transport studies using the cellular models (to be shown later).

Transcellular transport of Rh2s across Caco-2 cell monolayers

Before the transport study were performed, the transcellular transport of a prototypical substrate of p-glycoprotein (digoxin) was used as the positive control. The results showed that transcellular transport of digoxin displayed significant efflux ratio (21.1) and P_{a-b} was 0.74×10^{-6} cm/s, which was similar to the published results (Xu et al., 2003). In the presence of 20 μM cyclosporin A, the efflux ratio of digoxin was decreased to 1.2.

As expected, transcellular transport of Rh2s (2 μM) across Caco-2 monolayer from basolateral (B) to apical (A) side was significantly higher than the transport from A to B side, and the efflux ratios (P_{b-a} /P_{a-b}) were 28.5 (Table 1). Use of two MDR1/P-gp inhibitors alone at the apical side, 50 μM verapamil or 20 μM cyclosporin A, was able to completely inhibit the efflux

Downloaded from dmd.aspetjournals.org at ASPET Journals on April 18, 2024

DMD Fast Forward. Published on July 14, 2011 as DOI: 10.1124/dmd.111.040006
This article has not been copyedited and formatted. The final version may differ from this version.

transport of Rh2s, and the efflux ratio was decreased to close to 1. As expected, the P_{a-b} was significantly increased by 9 and 4 fold; and the P_{b-a} was significantly decreased by 3 and 6 fold after verapamil and cyclosporin A treatment, respectively (Table 1). Consistent with the permeability results, two p-glycoprotein inhibitors also significantly increased the intracellular accumulation of Rh2s following treatment with 50 µM verapamil (from 0.14 to 0.31 nmol/mg) or 20 µM cyclosporin A (from 0.14 to 0.54 nmol/mg).

Because there are three main efflux transporters (P-gp, MRP2 and BCRP) present at the apical membrane of the Caco-2 cells, chemical inhibitors of MRP2 (20 µM MK571) and BCRP (5 µM Ko143) were also used in transport study to determine their possible involvements. The inhibitors and inhibitor concentrations were chosen based on the reported Ki (constant of inhibition) value of 5.6 µM for MK571 (Walgren et al., 2000) and 0.6 µM for Ko143 (Brand et al., 2008) in the Caco-2 cells. Using the efflux ratio as the indicator of efflux transporter function, neither of these inhibitors was effective (Table 1). Similarly, the intracellular accumulations of Rh2s were not increased by either Ko143 or MK571, in line with the absence of the role of MRP2 or BCRP in limiting the uptake of Rh2s into Caco-2 cells (Table 1). Time-dependent transcellular transport of 2 µM Rh2s across monolayers of Caco-2 cells with different inhibitors were also presented in Supplemental Figure 2.

Downloaded from dmd.aspetjournals.org at ASPET Journals on April 18, 2024

Transcellular transport of Rh2s in MDR1- MDCKII cells

Human MDR1/P-gp over-expressing MDCKII cells were used to confirm the predominant role of P-gp in the transport of Rh2s. Prior to the transport studies of Rh2s, 2 µM digoxin was used as a positive control in MDR1-MDCKII cell transport study. The efflux ratio of digoxin was 64.0 in MDR1-MDCKII cell and the P_{a-b} is 2.98×10^{-7} cm/s, which was similar to the ratio reported in a previous publication (Taub et al., 2005).

DMD Fast Forward. Published on July 14, 2011 as DOI: 10.1124/dmd.111.040006
This article has not been copyedited and formatted. The final version may differ from this version.

The transport of Rh2s in parental MDCKII cells was used as a negative control since the cells have very low expression of P-gp (Shirasaka et al., 2009). As expected, the efflux ratio of Rh2s was much lower in parental MDCKII cells compared to MDR1-MDCKII cells at 2 μM (28.0 vs 2.4). Likewise, the P_{a-b} of Rh2s was more than 7 fold higher in the parental MDCKII cells (4.97×10^{-6} cm/s) than MDR1-MDCKII cells (0.68×10^{-6} cm/s) .

Four different concentrations of Rh2s were used in bi-directional transport study in MDR1-MDCKII cells and the efflux ratio was 65.7, 28.0, 12.4 and 6.7 at 1, 2, 3.3 and 5 μM, respectively (Table 1). The significantly decreased efflux ratios observed with increasing donor concentration of Rh2s ($p<0.05$) was due to an increased P_{a-b} value from 0.49×10^{-6} to 3.51×10^{-6} cm/s ($p<0.01$) and decreased P_{b-a} value from 32.77×10^{-6} to 23.5×10^{-6} cm/s.

Similar to the results of inhibition studies in Caco-2 cells, the presence of 20 μM cyclosporin A substantially decreased P_{b-a} (by 16 fold) and the efflux ratio (from 28.0 to 1.2) (Table 1).

The intracellular accumulations of Rh2s were also measured and the results showed that Rh2s accumulation was significantly higher (8.5 fold) in parental MDCKII cells (0.25 nmol/mg) than in MDR1-MDCKII cells (0.03 nmol/mg). Consistently, the intracellular accumulation of Rh2s was significantly increased by 20 fold ($p<0.001$), after co-incubation with CsA in MDR1- MDCKII cells (Table 1). Transcellular transport of Rh2s as a function of time across monolayers of parental MDCKII and MDR1- MDCKII cells at different concentrations and in the absence or presence of CsA were presented in Supplemental Figure 3.

Effects of MDR1 on the oral bioavailabilities of Rh2s

In order to investigate whether MDR1/P-gp has major effects on Rh2s oral bioavailability, plasma profiles of Rh2s were compared between MDR1a/b $^{-/-}$ and wild-type FVB mice after oral administration (20 mg/kg). In MDR1a/b $^{-/-}$ mice, the plasma C_{max} was significantly increased by

Downloaded from dmd.aspetjournals.org at ASPET Journals on April 18, 2024

DMD Fast Forward. Published on July 14, 2011 as DOI: 10.1124/dmd.111.040006
This article has not been copyedited and formatted. The final version may differ from this version.

17 fold ($p<0.01$) and $AUC_{0-\infty}$ was significantly increased by 23 fold ($p<0.001$) when compared to wild-type FVB mice (Fig 2, Table 2).

In MDR1a/b $^{-/-}$ mice, K_e was significantly decreased by 70% (from 0.50 ± 0.25 to 0.15 ± 0.02 hr^{-1}, $p<0.05$) compared to wild-type FVB mice. The $t_{1/2}$ of Rh2s was significantly increased by 2.5 fold (from 1.85 ± 1.27 to 4.60 ± 0.71 hr, $p<0.01$). The decreased K_e and increased $t_{1/2}$ could be attributed to the decreased elimination of Rh2s due to the knockout of the MDR1 gene (Table 2).

Effects of cyclosporin A on Rh2s oral bioavailabilities in A/J mice

Coadministration of the P-gp inhibitor, cyclosporin A (50 mg/kg), with Rh2s significantly increased the plasma C_{max} and $AUC_{0-\infty}$ of Rh2s at both 5 and 20 mg/kg (Fig. 3). The plasma C_{max} was significantly increased ($p<0.01$) by 14 fold at 5 mg/kg, and by 38 fold at 20 mg/kg. The plasma $AUC_{0-\infty}$ was significantly increased ($p<0.001$) by 36 fold at 5 mg/kg and 52 fold at 20 mg/kg. Pharmacokinetic parameters of Rh2s after i.v. administration were shown in Table 2 and the plasma $AUC_{0-\infty}$ from i.v. administration was used to calculate the absolute oral bioavailability for Rh2s. The absolute oral bioavailability of Rh2s was substantialy increased by 36 fold (from 0.94% to 33.18%, $p<0.001$) and 52 fold (from 0.52% to 27.14%, $p<0.001$) at 5 and 20 mg/kg, respectively.

Coadministration of cyclosporin A also decreased K_e by 2.8 fold (from 0.48 ± 0.25 to 0.17 ± 0.04 hr^{-1}, $p<0.05$) and 2 fold (from 0.32 ± 0.30 to 0.16 ± 0.03 hr^{-1}) at 5 and 20 mg/kg, respectively. Consistently, the half-life of Rh2s increased 78% (from 1.78 ± 0.90 to 4.41 ± 1.05 hr, $p<0.05$) and 36% (from 3.37± 1.78 to 4.60 ± 1.32 hr) at 5 and 20 mg/kg, respectively (Table 2).

Downloaded from dmd.aspetjournals.org at ASPET Journals on April 18, 2024

DMD Fast Forward. Published on July 14, 2011 as DOI: 10.1124/dmd.111.040006
This article has not been copyedited and formatted. The final version may differ from this version.

Co-administration of cyclosporin A also increased V_{ss} from 0.26 ± 0.24 to 0.49 ± 0.10 ($p<0.05$) L/Kg and 0.38 ±0.20 to 0.51 ± 0.12 ($p=0.2$) L/Kg at 5 and 20 mg/kg, although clearance of Rh2s was not changed after cyclosporin A treatment (Table 1).

In situ intestinal perfusion study of Rh2s

An intestinal perfusion study was performed to investigate intestinal absorption of Rh2s in A/J mice and MDR1 knockout FVB mice. Stability studies showed that Rh2s was stable in the intestinal perfusate for up to 8 hours (Supplemental Figure 4). Since the UPLC-MS/MS assay has approximate 10% standard deviation based on our validation data, accurate determination of %absorption was difficult if the absorption was poor (i.e., less than 10%). Percent absorption of Rh2s was higher in MDR1a/b $^{-/-}$ mice (64% and 14%) compared to WT FVB mice (<10%) in upper small intestine and colon, respectively. Similarly, percent absorption of Rh2s increased from <10% to 49.4% ($p<0.05$) in upper small intestine and from <10% to 19.8% in colon in the presence of 10 µM cyclosporin A in A/J mice (Fig. 4A). Consistently, the steady-state plasma concentration of Rh2s was significantly higher (0.80 µM) in MDR1a/b $^{-/-}$ mice than in WT FVB mice (0.13 µM) at the end of a 2.5 hour intestinal perfusion study. The steady-state plasma concentration of Rh2s was significantly increased by ~9 fold (from 0.12 µM to 1.07 µM, $p<0.05$) in the presence of 10 µM cyclosporin A in A/J mice (Fig. 4B).

Downloaded from dmd.aspetjournals.org at ASPET Journals on April 18, 2024

DMD Fast Forward. Published on July 14, 2011 as DOI: 10.1124/dmd.111.040006
This article has not been copyedited and formatted. The final version may differ from this version.

Discussion

This is the first comprehensive study that demonstrates unequivocally that Rh2s is a good substrate of P-gp, and P-gp mediates the efflux of Rh2s in vitro and in vivo. Although poor oral absorption of ginsenosides have been extensively reported, the results were mostly observational (Xie et al., 2005). One paper reported that Rh2s is not a substrate of P-gp because 10 μM verapamil did not decrease the efflux of Rh2s in the Caco-2 cell model (Zhang et al., 2010), which is contradictory to our conclusion. The discrepancy may be due to different P-gp expression level in Caco-2 cells among labs or the low concentration of inhibitor they used. Taken together, this means each model has its own limitation and we cannot rely on one single method to ascertain the transport mechanism of a substrate. Therefore, a series of studies ranging from *in vitro, in situ* and *in vivo* models were designed and conducted to support our conclusion that P-gp is the predominant efflux transporter responsible for Rh2s's poor bioavailability.

Our results showed that the other two apically located efflux transporters, MRP2 and BCRP, played a minimal role in the efflux of Rh2s. This conclusion was based on a lack of inhibition of Rh2s efflux or an absence of increase in intracellular accumulations of Rh2s in the presence of 20μM MK571 or 5 μM Ko143 in Caco-2 cells. Previously, we reported that 10μM MK571 significantly inhibited (by 61%) apical efflux of apigenin sulfate, which is a substrate of MRP2 in Caco-2 cells (Hu et al., 2003).

The results of this study clearly demonstrated that inhibition of P-gp by cyclosporin A and deletion of P-gp can substantially increase oral bioavailability of Rh2s. Consistent results in pharmacokinetic studies of Rh2s were observed in two strains of mice, FVB and A/J mice. FVB mice were used since the P-gp knockout mice were derived from this strain of mice. A/J mice were chosen in this paper because it was the strain used for lung cancer carcinogenesis and

Downloaded from dmd.aspetjournals.org at ASPET Journals on April 18, 2024

DMD Fast Forward. Published on July 14, 2011 as DOI: 10.1124/dmd.111.040006
This article has not been copyedited and formatted. The final version may differ from this version.

chemoprevention (Yan et al., 2007). The dominant role of P-gp in limiting the oral bioavailability of Rh2s was demonstrated by the facts that oral bioavailability of Rh2s was substantially increased (from 1% to above 30%) in A/J mice following cyclosporin A co-administration (Table 2), and that there were substantial increases in plasma C_{max} (17.2 fold) and $AUC_{0-\infty}$ (23.0 fold) in MDR1a/b $^{-/-}$ mice compared to WT FVB mice. The improved bioavailability of Rh2s in the presence of a P-gp inhibitor was mainly attributed to enhanced intestinal absorption in mice based on the intestinal perfusion study (Fig. 4). Mechanisms responsible for increased absorption were likely to be increased permeability and elevated intracellular accumulations, as shown in both Caco-2 and MDR1-MDCKII cell models (Table 1). The improved bioavailability could also be contributed by decreased elimination, as indicated by a slower elimination rate constant (k_e) and a prolonged terminal half-life.

The extremely poor oral bioavailability of Rh2s (<1%) was consistent with its low solubility and low permeability observed in this study, suggesting that Rh2s belongs to the class IV compounds in the BCS classification system (Dahan et al., 2009). However, the apparent low permeability of Rh2s is due to efflux by P-gp, since its intrinsic permeability (passive diffusion) is promising with the highest P_{a-b} exceeding $3x10^{-6}$ cm/sec (obtained in the presence of P-gp inhibitors) (Table 1). The substantial increase in oral bioavailability of Rh2s in the presence of cyclosporin A to a level above 30% suggests that this compound holds great promise for oral administration (necessary for cancer chemoprevention) if it is properly formulated. Therefore, we have shown that it is possible to derive good oral bioavailability for Rh2s in animals as long as we can inhibit the function of P-gp during absorption.

We have shown that inhibition or deletion of P-gp was the main reason for improved Rh2s bioavailability in mice. In demonstrating the large changes in oral bioavailability of Rh2s, we have seen some minor inconsistency. For example, the AUC value of Rh2s (20 mg/kg) in cyclosporin A treatment group in A/J mice was higher than that in the MDR1a/b $^{-/-}$ FVB mice. It

Downloaded from dmd.aspetjournals.org at ASPET Journals on April 18, 2024

DMD Fast Forward. Published on July 14, 2011 as DOI: 10.1124/dmd.111.040006
This article has not been copyedited and formatted. The final version may differ from this version.

was likely due to strain differences in absorption and/or clearance of this compound. Additional factors such as difference in CYP metabolism of Rh2s were also possible. We believed that a major contribution from CYP was less likely since CYP metabolites of Rh2s were never reported except its hydrolysis product (aglycone) in vivo (Qian et al., 2005). In addition, the large differences in C_{max} and AUC values existed between FVB control and MDR1a/b $^{-/-}$ FVB mice were comparable to those achieved with P-gp inhibition by cyclosporin A in A/J mice. However, the contribution from CYP cannot be excluded since other ginsenosides with similar structures were reported as substrates of CYP enzyme (Hao et al., 2010), and cyclosporin A is also a potent inhibitor of CYP.

We did not observe an increase in oral bioavailabilty of Rh2s at the higher dose (in absence of P-gp inhibitor) as expected since efflux ratios were smaller at higher concentrations (Table 1). We hypothesized that poor solubility was the reason that this enhancment did not occur. This is because ginsenosides with less sugar moiety (e.g., protopanaxadiol, protopanaxtriol, Rh2, and Rg3) usually have poor aqueous solubilities (Gu et al., 2010). Our solubility study showed the low aqueous solubility of Rh2s (~3 µg/ml at pH 7.4) in HBSS buffer, (~5 µg/ml at pH 7.4) in water and (~7 µg/ml at pH 6.8) in SIF. The poor aqueous solubility of Rh2s further substantiates the important role of P-gp efflux in vivo since Rh2s cannot fully saturate/inhibit P-gp efflux in lumen due to limited and low solubility. This result did not contradict the results reported by Zhang et al, who showed that Rh2s suspended in sodium CMC could act as an P-gp inhibitor at 25 mg/kg in rats (Zhang et al., 2010), but it did signify that unformulated Rh2s is probably not a very useful P-gp inhibitor in vivo due to solubility limit. Further studies are planned to determine how solubilization of Rh2s could be used to further increase its bioavailability when used together with a P-gp inhibitor.

This proof of principle study demonstrated that oral bioavailability of Rh2s can be enhanced to a clinically acceptable level (30%) if P-gp function is completely inhibited. Since many potent

Downloaded from dmd.aspetjournals.org at ASPET Journals on April 18, 2024

DMD Fast Forward. Published on July 14, 2011 as DOI: 10.1124/dmd.111.040006
This article has not been copyedited and formatted. The final version may differ from this version.

ginsenosides were also showed to be substrates of P-gp in Caco-2 and MDR1-MDCKII cells (unpublished data), P-gp efflux appeared to be an important mechanism responsible for their low bioavailabilities. These results may therefore redefine our understanding on absorption of potent ginsenosides, and point to a strategy to increase their oral bioavailability so their clinical potentials can be fully evaluated. However, cyclosporin A is not an ideal P-gp inhibitor for continuous clinical usage in healthy humans due to its known therapeutic and adverse effects. Further studies are ongoing to screen other less pharmacologically active compound that may serve as potent P-gp inhibitors to enhance oral bioavailability of Rh2s.

In summary, we demonstrated clearly that Rh2s is a good substrate of P-gp both in vitro and in vivo, and that effective and efficient inhibition of P-gp by cyclosporin A led to an increased oral bioavailability of Rh2s in A/J mice. The conclusion is supported by the facts that (1) deletion of P-gp functionality (as in MDR1a/b$^{-/-}$ FVB mice) significantly increases the oral absorption and bioavailability of Rh2s; and (2) inhibition of efflux transporter P-gp substantially increases cellular uptake and transcellular transport of Rh2s in Caco-2 and MDR1-MDCKII cells. Additional studies are currently ongoing to search for P-gp inhibitors that are effective and clinically applicable for long-term use.

Downloaded from dmd.aspetjournals.org at ASPET Journals on April 18, 2024

DMD Fast Forward. Published on July 14, 2011 as DOI: 10.1124/dmd.111.040006
This article has not been copyedited and formatted. The final version may differ from this version.

Acknowledgements

The pharmacokinetic data analysis was assisted by Dr. Diana Chow in College of Pharmacy, University of Houston.

Downloaded from dmd.aspetjournals.org at ASPET Journals on April 18, 2024

DMD Fast Forward. Published on July 14, 2011 as DOI: 10.1124/dmd.111.040006
This article has not been copyedited and formatted. The final version may differ from this version.

Authorship Contributions

Participated in research design: Yang, Gao and Hu.

Conducted experiments: Yang, Gao, Yin, Wang, and Teng.

Contributed new reagents or analytic tools: You and Jiang

Performed data analysis: Yang, Teng, Wang, Wu and Hu.

Wrote or contributed to the writing of the manuscript: Yang and Hu.

Downloaded from dmd.aspetjournals.org at ASPET Journals on April 18, 2024

DMD Fast Forward. Published on July 14, 2011 as DOI: 10.1124/dmd.111.040006
This article has not been copyedited and formatted. The final version may differ from this version.

References

Aller SG, Yu J, Ward A, Weng Y, Chittaboina S, Zhuo R, Harrell PM, Trinh YT, Zhang Q, Urbatsch IL and Chang G (2009) Structure of P-glycoprotein reveals a molecular basis for poly-specific drug binding. *Science* **323:**1718-1722.

Brand W, van der Wel PA, Rein MJ, Barron D, Williamson G, van Bladeren PJ and Rietjens IM (2008) Metabolism and transport of the citrus flavonoid hesperetin in Caco-2 cell monolayers. *Drug Metab Dispos* **36:**1794-1802.

Buettner C, Yeh GY, Phillips RS, Mittleman MA and Kaptchuk TJ (2006) Systematic review of the effects of ginseng on cardiovascular risk factors. *Ann Pharmacother* **40:**83-95.

Cheng CC, Yang SM, Huang CY, Chen JC, Chang WM and Hsu SL (2005) Molecular mechanisms of ginsenoside Rh2-mediated G1 growth arrest and apoptosis in human lung adenocarcinoma A549 cells. *Cancer Chemother Pharmacol* **55:**531-540.

Christensen LP (2009) Ginsenosides chemistry, biosynthesis, analysis, and potential health effects. *Adv Food Nutr Res* **55:**1-99.

Coleman CI, Hebert JH and Reddy P (2003) The effects of Panax ginseng on quality of life. *J Clin Pharm Ther* **28:**5-15.

Dahan A, Miller JM and Amidon GL (2009) Prediction of solubility and permeability class membership: provisional BCS classification of the world's top oral drugs. *AAPS J* **11:**740-746.

Gu Y, Wang GJ, Sun JG, Jia YW, Wang W, Xu MJ, Lv T, Zheng YT and Sai Y (2009) Pharmacokinetic characterization of ginsenoside Rh2, an anticancer nutrient from ginseng, in rats and dogs. *Food Chem Toxicol* **47:**2257-2268.

Gu Y, Wang GJ, Wu XL, Zheng YT, Zhang JW, Ai H, Sun JG and Jia YW (2010) Intestinal absorption mechanisms of ginsenoside Rh2: stereoselectivity and involvement of ABC transporters. *Xenobiotica* **40:**602-612.

Hao H, Lai L, Zheng C, Wang Q, Yu G, Zhou X, Wu L, Gong P and Wang G (2010) Microsomal cytochrome p450-mediated metabolism of protopanaxatriol ginsenosides: metabolite profile, reaction phenotyping, and structure-metabolism relationship. *Drug Metab Dispos* **38:**1731-1739.

Helms S (2004) Cancer prevention and therapeutics: Panax ginseng. *Altern Med Rev* **9:**259-274.

Hu M, Chen J and Lin H (2003) Metabolism of flavonoids via enteric recycling: mechanistic studies of disposition of apigenin in the Caco-2 cell culture model. *J Pharmacol Exp Ther* **307:**314-321.

Jeong EJ, Jia X and Hu M (2005) Disposition of formononetin via enteric recycling: metabolism and excretion in mouse intestinal perfusion and Caco-2 cell models. *Mol Pharm* **2:**319-328.

Jia L, Zhao Y and Liang XJ (2009) Current evaluation of the millennium phytomedicine- ginseng (II): Collected chemical entities, modern pharmacology, and clinical applications emanated from traditional Chinese medicine. *Curr Med Chem* **16:**2924-2942.

Kemper EM, Cleypool C, Boogerd W, Beijnen JH and van Tellingen O (2004) The influence of the P-glycoprotein inhibitor zosuquidar trihydrochloride (LY335979) on the brain penetration of paclitaxel in mice. *Cancer Chemother Pharmacol* **53:**173-178.

Kusuhara H and Sugiyama Y (2002) Role of transporters in the tissue-selective distribution and elimination of drugs: transporters in the liver, small intestine, brain and kidney. *J Control Release* **78:**43-54.

Downloaded from dmd.aspetjournals.org at ASPET Journals on April 18, 2024

DMD Fast Forward. Published on July 14, 2011 as DOI: 10.1124/dmd.111.040006
This article has not been copyedited and formatted. The final version may differ from this version.

Liu H, Yang J, Du F, Gao X, Ma X, Huang Y, Xu F, Niu W, Wang F, Mao Y, Sun Y, Lu T, Liu C, Zhang B and Li C (2009) Absorption and disposition of ginsenosides after oral administration of Panax notoginseng extract to rats. *Drug Metab Dispos* **37:**2290-2298.

Meerum Terwogt JM, Beijnen JH, ten Bokkel Huinink WW, Rosing H and Schellens JH (1998) Co-administration of cyclosporin enables oral therapy with paclitaxel. *Lancet* **352:**285.

Qian T, Cai Z, Wong RN and Jiang ZH (2005) Liquid chromatography/mass spectrometric analysis of rat samples for in vivo metabolism and pharmacokinetic studies of ginsenoside Rh2. *Rapid Commun Mass Spectrom* **19:**3549-3554.

Sharom FJ (2008) ABC multidrug transporters: structure, function and role in chemoresistance. *Pharmacogenomics* **9:**105-127.

Shirasaka Y, Konishi R, Funami N, Kadowaki Y, Nagai Y, Sakaeda T and Yamashita S (2009) Expression levels of human P-glycoprotein in in vitro cell lines: correlation between mRNA and protein levels for P-glycoprotein expressed in cells. *Biopharm Drug Dispos* **30:**149-152.

Taub ME, Podila L, Ely D and Almeida I (2005) Functional assessment of multiple P-glycoprotein (P-gp) probe substrates: influence of cell line and modulator concentration on P-gp activity. *Drug Metab Dispos* **33:**1679-1687.

van Waterschoot RA, Lagas JS, Wagenaar E, van der Kruijssen CM, van Herwaarden AE, Song JY, Rooswinkel RW, van Tellingen O, Rosing H, Beijnen JH and Schinkel AH (2009) Absence of both cytochrome P450 3A and P-glycoprotein dramatically increases docetaxel oral bioavailability and risk of intestinal toxicity. *Cancer Res* **69:**8996-9002.

Varjas T, Nowrasteh G, Budan F, Nadasi E, Horvath G, Makai S, Gracza T, Cseh J and Ember I (2009) Chemopreventive effect of Panax ginseng. *Phytother Res* **23:**1399-1403.

Walgren RA, Karnaky KJ, Jr., Lindenmayer GE and Walle T (2000) Efflux of dietary flavonoid quercetin 4'-beta-glucoside across human intestinal Caco-2 cell monolayers by apical multidrug resistance-associated protein-2. *J Pharmacol Exp Ther* **294:**830-836.

Wang Z, Zheng Q, Liu K, Li G and Zheng R (2006) Ginsenoside Rh(2) enhances antitumour activity and decreases genotoxic effect of cyclophosphamide. *Basic Clin Pharmacol Toxicol* **98:**411-415.

Xie HT, Wang GJ, Chen M, Jiang XL, Li H, Lv H, Huang CR, Wang R and Roberts M (2005) Uptake and metabolism of ginsenoside Rh2 and its aglycon protopanaxadiol by Caco-2 cells. *Biol Pharm Bull* **28:**383-386.

Xu J, Go ML and Lim LY (2003) Modulation of digoxin transport across Caco-2 cell monolayers by citrus fruit juices: lime, lemon, grapefruit, and pummelo. *Pharm Res* **20:**169-176.

Yan Y, Cook J, McQuillan J, Zhang G, Hitzman CJ, Wang Y, Wiedmann TS and You M (2007) Chemopreventive effect of aerosolized polyphenon E on lung tumorigenesis in A/J mice. *Neoplasia* **9:**401-405.

Yang Z, Gao S, Yin T, Kulkarni KH, Teng Y, You M and Hu M (2010a) Biopharmaceutical and pharmacokinetic characterization of matrine as determined by a sensitive and robust UPLC-MS/MS method. *J Pharm Biomed Anal* **51:**1120-1127.

Yang Z, Zhu W, Gao S, Xu H, Wu B, Kulkarni K, Singh R, Tang L and Hu M (2010b) Simultaneous determination of genistein and its four phase II metabolites in blood by a sensitive and robust UPLC-MS/MS method: Application to an oral bioavailability study of genistein in mice. *J Pharm Biomed Anal* **53:**81-89.

Yun TK (1996) Experimental and epidemiological evidence of the cancer-preventive effects of Panax ginseng C.A. Meyer. *Nutr Rev* **54:**S71-81.

Yun TK (2003) Experimental and epidemiological evidence on non-organ specific cancer preventive effect of Korean ginseng and identification of active compounds. *Mutat Res* **523-524:**63-74.

Downloaded from dmd.aspetjournals.org at ASPET Journals on April 18, 2024

DMD Fast Forward. Published on July 14, 2011 as DOI: 10.1124/dmd.111.040006
This article has not been copyedited and formatted. The final version may differ from this version.

Zhang J, Zhou F, Wu X, Gu Y, Ai H, Zheng Y, Li Y, Zhang X, Hao G, Sun J, Peng Y and Wang G (2010) 20(S)-Ginsenoside Rh2 noncompetitively inhibits P-glycoprotein in vitro and in vivo: a case for herb-drug interactions. *Drug Metab Dispos* **12:**2179-2187.

Downloaded from dmd.aspetjournals.org at ASPET Journals on April 18, 2024

DMD Fast Forward. Published on July 14, 2011 as DOI: 10.1124/dmd.111.040006
This article has not been copyedited and formatted. The final version may differ from this version.

Figure Legends

Figure 1. Chemical structure of 20(s)-ginsenoside Rh2 (Molecular weight: 622).

Figure 2. The plasma concentrations of Rh2s in wild-type and MDR1a/b $^{-/-}$ FVB mice after oral administration at 20 mg/kg. Data are presented as mean ± S.D.; n=5.

Figure 3. The plasma concentrations of Rh2s alone or with 50 mg/kg cyclosporin A (CsA) treatment after oral administrations at 5 and 20 mg/kg in A/J mice. Data are presented as mean ± S.D.; n=5.

Note: 12 hours samples for 20 mg/kg with CsA treatment group were not collected. The point in the circle represents the average concentration, which is an approximate value since not all samples contained quantifiable Rh2s.

Figure 4. (A) The absorption percentages of Rh2s (2 μM) in intestinal perfusion in WT, MDR1a/b $^{-/-}$ FVB and A/J mice. (B) The plasma concentrations of Rh2s after intestinal perfusion in WT, MDR1a/b $^{-/-}$ FVB and A/J mice. 10 μM CsA were added in perfusate to inhibit P-gp function in A/J mice. Data are presented as mean ± S.D.; n=4.

* indicated $p<0.05$.

indicated the absorption percentages of Rh2s were less than 10%.

Downloaded from dmd.aspetjournals.org at ASPET Journals on April 18, 2024

Table 1. Transcellular transport of Rh2s across monolayers of Caco-2, MDCKII, and MDR1-MDCKII cells in the absence or presence of inhibitors.

Data are presented as mean ± S.D; n=3.

Cell model	Substrate concentration (μM)	Inhibitor	Inhibitor concentration (μM)	P_{a-b} ($\times10^{-6}$ cm/s)	P_{b-a} ($\times10^{-6}$ cm/s)	Efflux ratio (P_{b-a}/P_{a-b})	Intracellular amounts (nmol/mg)
Caco-2	2	-	-	0.37±0.01	10.66±1.74	28.5±4.7	0.14±0.02
		Verapamil	50	3.21±0.35*	3.25±0.46*	1.0±0.1*	0.31±0.04**
		Cyclosporin A	20	1.42±0.18*	1.71±0.23*	1.2±0.2*	0.54±0.08**
		KO143	5	0.39±0.13	8.97±2.40	22.7±6.1	0.13±0.02
		MK571	20	0.39±0.34	16.01±1.46	41.1±4.0	0.33±0.20
MDCK II	2	-	-	4.97±0.69	11.97±2.40	2.4±0.5	0.25±0.09
MDR1-MDCKII	1	-	-	0.49±0.06	32.77±3.33	65.7±6.7	0.06±0
	2			0.68±0.21	19.16±4.92	28.0±7.2	0.03±0.02
	3.3			2.17±0.39	26.79±2.77	12.4±1.3	0.19±0.05
	5			3.51±0.73	23.50±1.93	6.7±0.6	0.67±0.14
	2	Cyclosporin A	20	0.84±0.14	1.19±0.21**	1.4±0.2*	0.61±0.09***

"P_{a-b}" refers to the permeability from apical to basolateral and "P_{b-a}" refers to the permeability from basolateral to apical side. Permeability, ER and intracellular amounts were compared to control group. Data are the means ± S.D. of three independent experiments.

– indicated no inhibitor; * indicated $p<0.05$; ** indicated $p<0.01$; *** indicated $p<0.001$.

Downloaded from dmd.aspetjournals.org at ASPET Journals on April 18, 2024

DMD Fast Forward. Published on July 14, 2011 as DOI: 10.1124/dmd.111.040006
This article has not been copyedited and formatted. The final version may differ from this version.

Table 2. The pharmacokinetic parameters of Rh2s in A/J, FVB and MDR1a/b $^{-/-}$ mice at different doses following different routes of administration. Data are presented as mean ± S.D; n=5.

Animal Strain	Route/Dose	Inhibitor (CsA)	T_{max} (hr)	C_{max} (μM)	k_e (hr^{-1})	$t_{1/2}$ (hr)	V_{ss} (L/Kg)	CL (L/hr/Kg)	AUC $_{0-\infty}$ (hr*μM)	F (%)
A/J	i.v. 5mg/kg	-	-	-	0.40± 0.09	1.77± 0.37	0.36± 0.22	0.13± 0.06	98.52± 45.58	-
	p.o. 5mg/kg	-	2.80± 0.84	0.31± 0.30	0.48± 0.25	1.78± 0.90	0.26± 0.24	0.07± 0.01	0.92± 0.90	0.94± 0.92
	p.o. 5mg/kg	50mg/kg	6.50± 1.91*	4.46± 1.20***	0.17± 0.04*	4.41± 1.05**	0.49± 0.10*	0.08± 0	32.69± 4.92***	33.18± 4.99***
	p.o. 20mg/kg	-	4.17± 1.60	0.28± 0.10	0.32± 0.30	3.37± 1.78	0.38± 0.20	0.08± 0	2.04± 1.50	0.52± 0.38
	p.o. 20mg/kg	50mg/kg	4.60± 1.34	10.66± 1.35***	0.16± 0.03	4.60± 1.32	0.51± 0.12	0.08± 0	106.97± 26.02***	27.14± 6.60***
Wild type FVB	p.o. 20mg/kg	-	3.04± 2.70	0.35± 0.36	0.50± 0.25	1.85± 1.27	-	-	2.17± 3.42	-
MDR1a/b $^{-/-}$ FVB	p.o. 20mg/kg	-	4.25± 2.50*	6.01± 1.89**	0.15± 0.02*	4.60± 0.71*	-	-	49.90± 3.20***	-

Pharmacokinetic parameters of Rh2s in cyclosporin A (CsA) co-administration group were compared to Rh2s alone group at the same dose; and pharmacokinetic parameters of Rh2s in MDR1a/b $^{-/-}$mice group were compared to wild-type FVB mice group

* indicated p<0.05; ** indicated p<0.01; *** indicated p<0.001.

Downloaded from dmd.aspetjournals.org at ASPET Journals on April 18, 2024

DMD Fast Forward. Published on July 14, 2011 as DOI: 10.1124/dmd.111.040006
This article has not been copyedited and formatted. The final version may differ from this version.

Note: V_{ss} and CL are not available in wt FVB and MDR1 knockout mice due to unknown oral bioavailability of Rh2s after oral administration.

DMD Fast Forward. Published on July 14, 2011 as DOI: 10.1124/dmd.111.040006
This article has not been copyedited and formatted. The final version may differ from this version.

Downloaded from dmd.aspetjournals.org at ASPET Journals on April 18, 2024

DMD Fast Forward. Published on July 14, 2011 as DOI: 10.1124/dmd.111.040006
This article has not been copyedited and formatted. The final version may differ from this version.

Figure 1

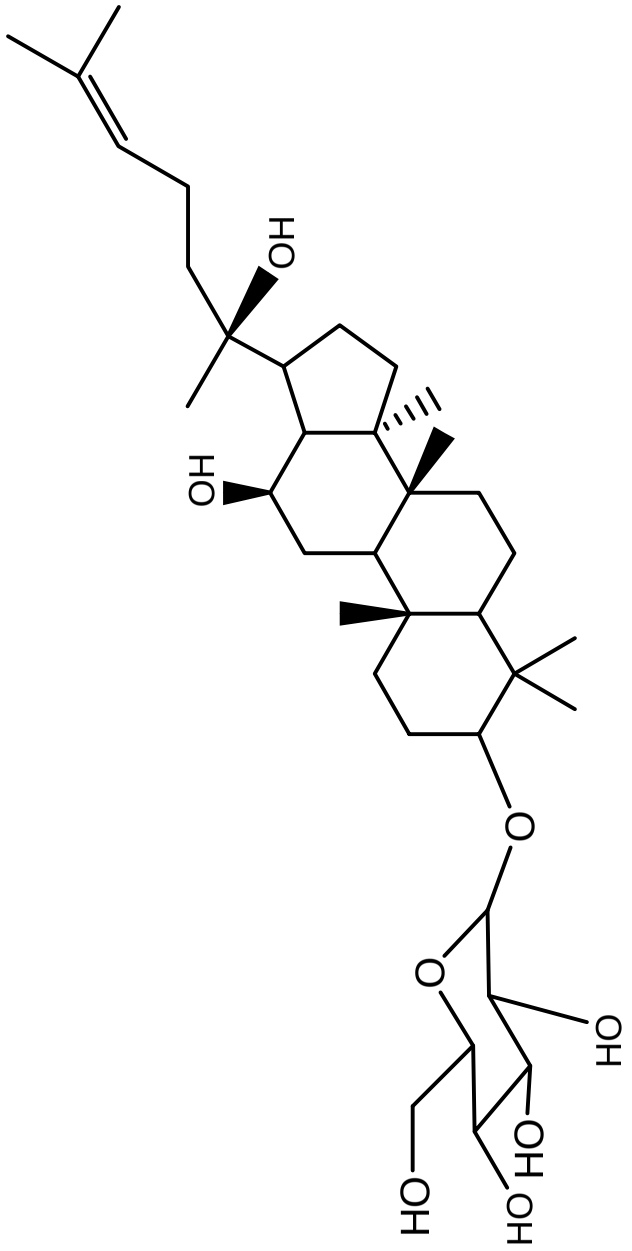

Downloaded from dmd.aspetjournals.org at ASPET Journals on April 18, 2024

Figure 2

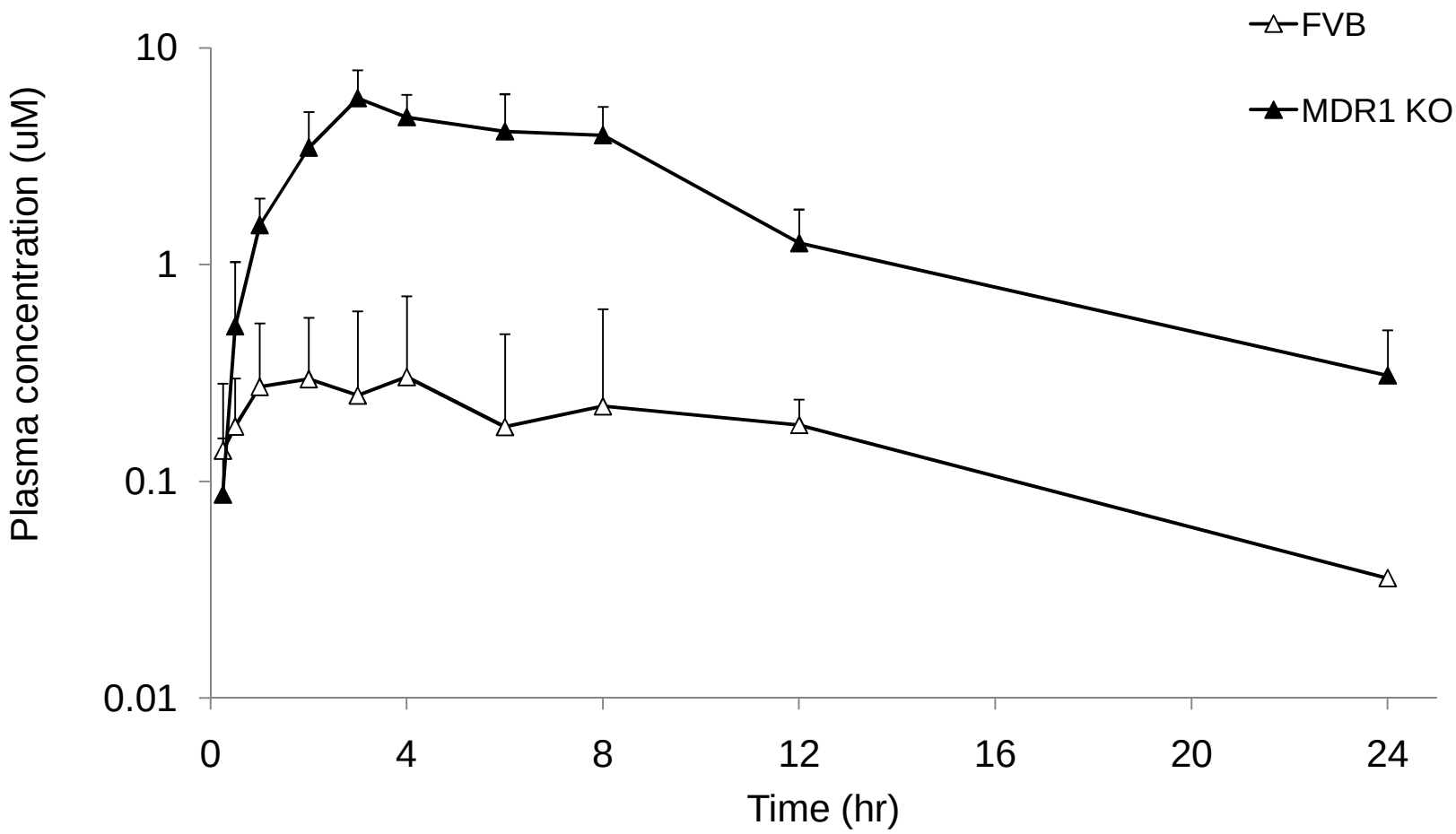

DMD Fast Forward. Published on July 14, 2011 as DOI: 10.1124/dmd.111.040006
This article has not been copyedited and formatted. The final version may differ from this version.

Downloaded from dmd.aspetjournals.org at ASPET Journals on April 18, 2024

Figure 3

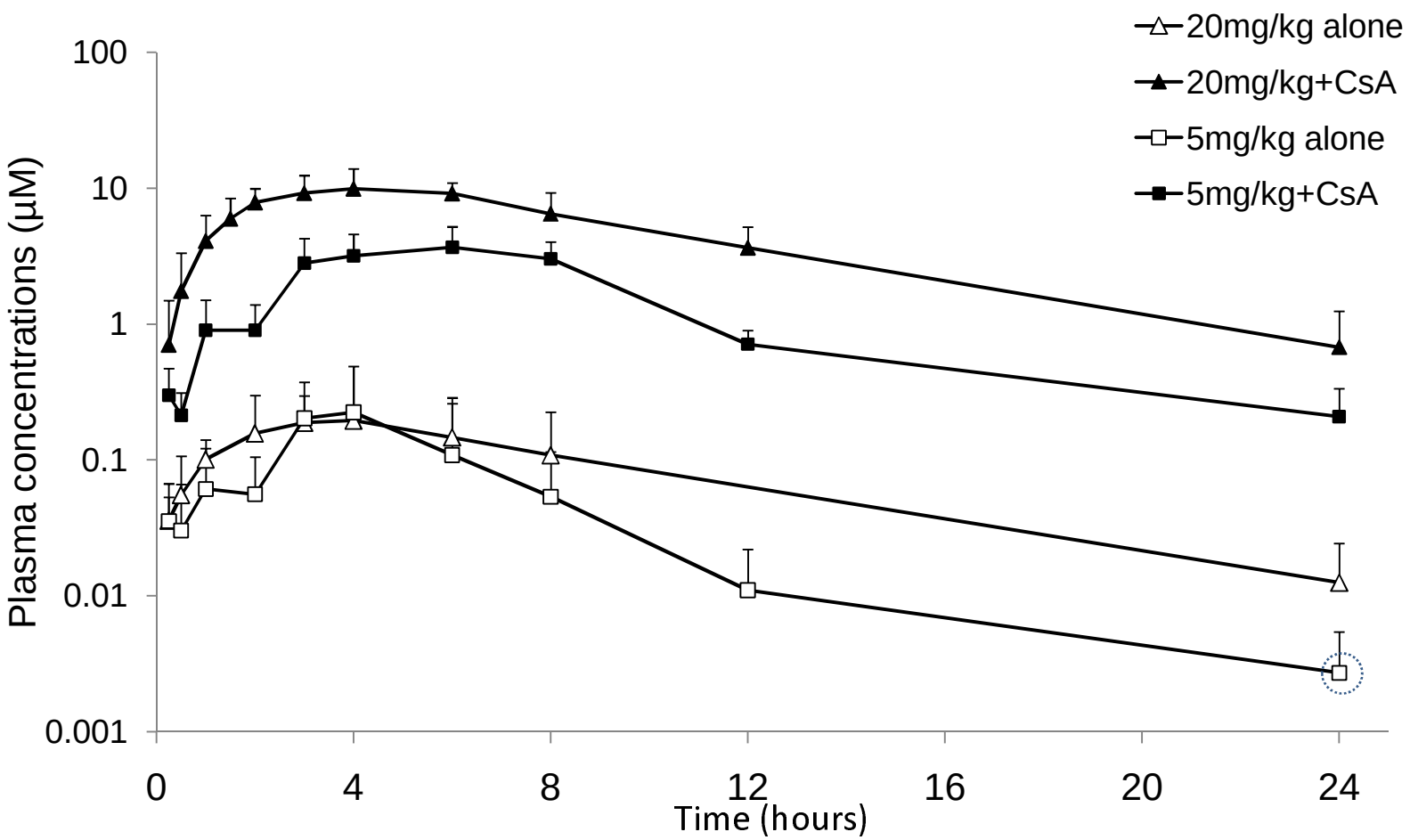

DMD Fast Forward. Published on July 14, 2011 as DOI: 10.1124/dmd.111.040006
This article has not been copyedited and formatted. The final version may differ from this version.

Downloaded from dmd.aspetjournals.org at ASPET Journals on April 18, 2024

Figure 4

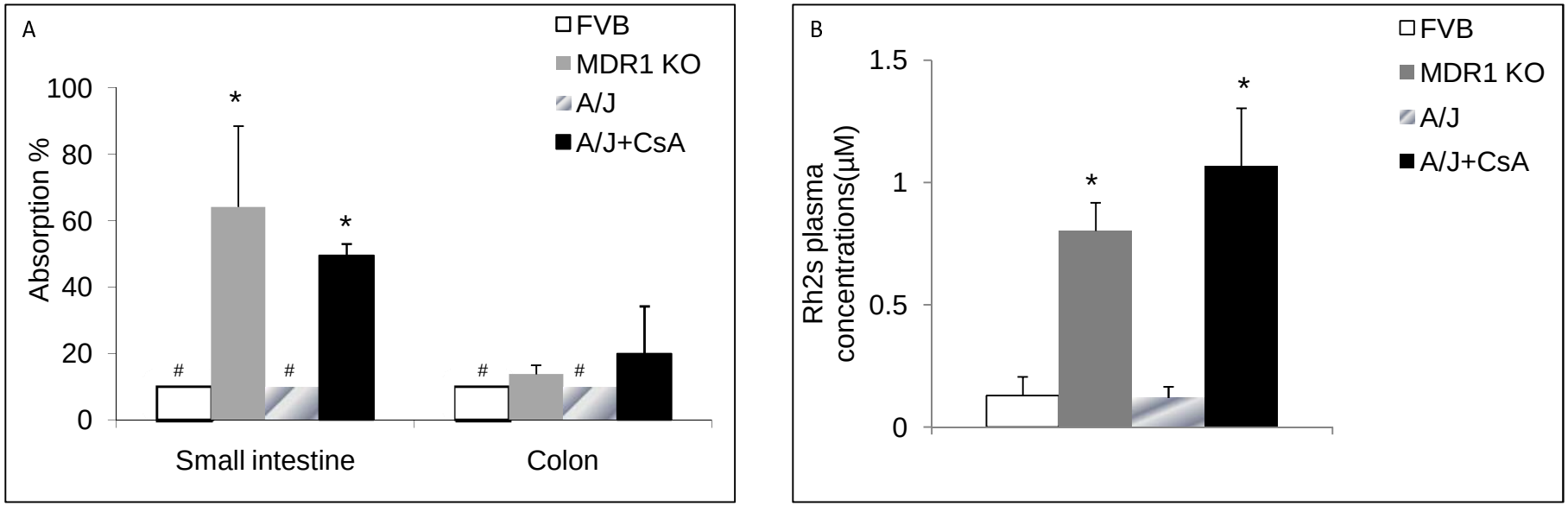

DMD Fast Forward. Published on July 14, 2011 as DOI: 10.1124/dmd.111.040006
This article has not been copyedited and formatted. The final version may differ from this version.

Downloaded from dmd.aspetjournals.org at ASPET Journals on April 18, 2024